



POLITECNICO DI TORINO
Repository ISTITUZIONALE

Utilizing Base-isolation Systems to Increase Earthquake Resiliency of Healthcare and School Buildings

Original

Utilizing Base-isolation Systems to Increase Earthquake Resiliency of Healthcare and School Buildings / Moretti, Sarah; Trozzo, Alba; Terzic, Vesna; Cimellaro, Gian Paolo; Mahin, Stephen. - In: PROCEDIA ECONOMICS AND FINANCE. - ISSN 2212-5671. - ELETTRONICO. - 18(2014), pp. 969-976.

Availability:

This version is available at: 11583/2652908 since: 2016-11-21T16:29:28Z

Publisher:

Elsevier

Published

DOI:10.1016/S2212-5671(14)01024-7

Terms of use:

openAccess

This article is made available under terms and conditions as specified in the corresponding bibliographic description in the repository

Publisher copyright

(Article begins on next page)



4th International Conference on Building Resilience, Building Resilience 2014, 8-10 September
2014, Salford Quays, United Kingdom

Utilizing base-isolation systems to increase earthquake resiliency of healthcare and school buildings

Sarah Moretti¹, Vesna Terzic², Gian Paolo Cimellaro^{1*}, Stephen Mahin²

*1: Politecnico di Torino, Department of Structural, Geotechnical & Building Engineering (DISEG), Turin, Italy,
2: University of California, Berkeley, Department of Civil and Environmental Engineering, Berkeley, California, USA*

Do not include author information – double blind peer review Abstract

In the recent large earthquakes in Chile, New Zealand, and Japan, a great number of critical facilities, including hospitals, schools, bridges, factories, airports, and utility systems, experienced extensive damage resulting in their loss of their function, and consequently substantial economic losses. Heavily affected communities were paralyzed for months following these large seismic events. The recovery process is estimated to last from several years to few decades. As a result, increased attention is being placed on strategies to design facilities that are both safe and damage resistant. It is often presumed that such an approach increases costs to an unacceptable level. The study reported herein compares the repair costs and repair times considering two designs for a typical three-story steel building: conventional fixed-base and damage resistant base-isolated moment resisting frame system. Performance-based earthquake evaluation tools are used to estimate repair costs and times for five different hazard levels considering two occupancy types critical for recovery: healthcare and school. The buildings are located in a seismically active region of western North America. It is demonstrated that using seismic isolation to enhance damage resistance results in significantly smaller repair cost, repair time, and improved resilience for the base-isolated alternative compared to a conventional fixed-base design.

© 2014 The Authors. Published by Elsevier B.V.

Selection and/or peer-reviewed under responsibility of the Centre for Disaster Resilience, School of the Built Environment, University of Salford.

Keywords: Resilience, Hospital performance, seismic performance, repair cost, downtime, life-cycle losses

* Corresponding author. Tel.: +39 338 6274741; fax: +39 011 090 4899.
E-mail address: gianpaolo.cimellaro@polito.it

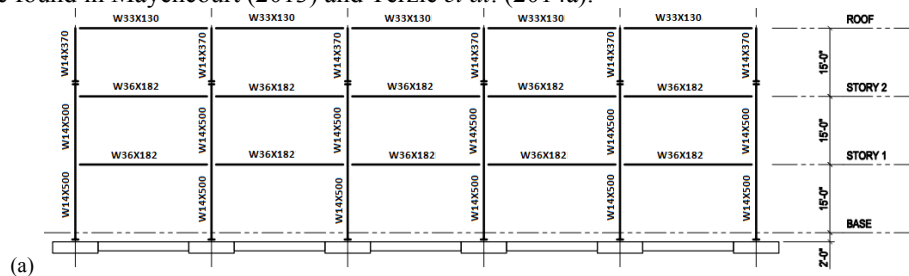
1. Introduction

Healthcare facilities and schools represent a substantial hazard to human life in the event of failure (occupancy category III, per ICC IBC, 2012). Therefore, they are designed following more stringent design requirements than buildings with residential and commercial occupancy. In the recent large earthquakes in Chile, New Zealand, and Japan, healthcare facilities and schools were generally safe. However, there are evidences of healthcare and school closures due to extensive structural and nonstructural damage that resulted in the loss of their function (Miranda et al., 2012). As a result, increased attention is being placed on strategies to design facilities that are both safe and damage resistant. It is often presumed that such an approach increases costs to an unacceptable level. However, the cost-effectiveness of alternative design choices can be assessed using performance-based earthquake evaluation (PBEE) methods (Miranda, 2003) that quantify expected future costs associated with damage repair, loss of functionality, casualties, and so on.

This paper presents results of a study that compares the repair costs and repair times considering two designs for a three-story steel building: high performance special moment resisting frame (HP-SMRF) and damage resistant base-isolated intermediate moment resisting frame (BI-IMRF). Both system's designs comply with the occupancy category III (ICC IBC, 2012), allowing the building to serve either as a healthcare facility or as a school. To aid understanding of the relative performance of these two systems considering the two occupancy types, key engineering demand parameters (i.e., median values of maximum and residual story drifts and floor accelerations), repair costs, and repair times are compared at five hazard levels. These results are then used to estimate the resilience of the two systems. Finally, the value of PBEE analysis in identifying cost-effective seismic design strategies that produce more resilient, damage-resistant structures is discussed.

2. Buildings description

The study considered a three-story steel building located in Oakland, California, a site representative of the high seismic hazard characteristics of western North America. The basic building plan dimensions are 120 ft (36.5 m) by 180 ft (54.9 m) with a bay spacing of 30 ft (9.1 m) in each direction. The building is located on relatively stiff soil (site class C/D with reference shear wave velocity = 180 to 360 m/s). Code spectral accelerations were selected to be $S_s = 2.2g$ for short periods and $S_1 = 0.74g$ at a period of 1 sec, which are representative of many locations in California. The designs of the two considered systems, fixed-base and base-isolated moment resisting frames, are consistent with what might be used by many engineers and are compliant with the code standards for design according to the Equivalent Lateral Force Method (ASCE, 2010). The HP-SMRF [Fig. 1(a)] was designed with a force reduction factor (R/I_e) of 6.4 (8/1.25), an interstory drift limit of 1.0% (more stringent than 2% required by code – ASCE, 2010), and utilized prequalified WUF-W beam-to-column connections (AISC, 2005). Such design resulted in fundamental period of the fixed-base system of 0.67 sec. Compared to the HP-SMRF, the BI-IMRF [Fig. 1(b)] was designed utilizing lower R/I_e factor ($1.69=(3/8) \times (4.5/1)$) and the same drift limit (1.0%). The IMRF uses simpler connection details and does not require a strong column-weak girder design approach. The isolation system is designed to have a maximum displacement of 30 in. under the maximum capable earthquake (MCE) event. It utilizes triple friction pendulum bearings (TFPB) with the friction coefficients of the four sliding surfaces of 0.01, 0.01, 0.03, and 0.06, and the effective pendulum lengths of 20, 122, and 122 in. Under the MCE event, this bearing has the effective period of 4.35 sec and the effective damping of 15.1%. More details on designs of these two systems can be found in Mayencourt (2013) and Terzic *et al.* (2014a).



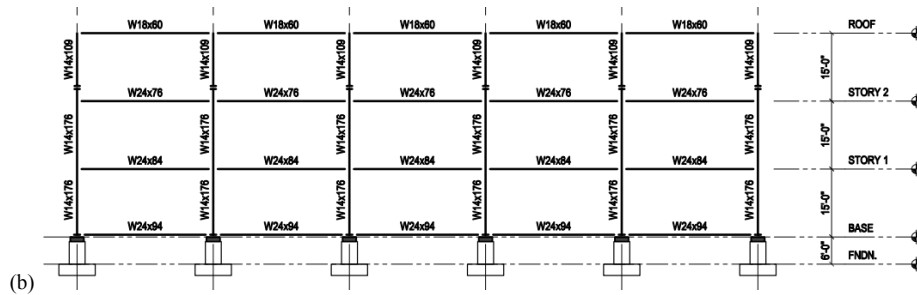


Fig. 1. Lateral force resisting systems configurations (a) HP-SMRF and (b) BI-IMRF.

3. Ground motion selection

The set of ground motions used in the analysis were selected to match the uniform hazard spectrum (USGS, 2013) and associated causal events for the Oakland site. Forty three-component ground motion records were selected to represent the ground motion hazard at each of three hazard levels: 2%, 10%, and 50% probabilities of exceedence in 50 years. More information on these motions can be found in Baker *et al.* (2011). To better characterize the seismic hazard at the site, two additional sets of ground motion records representative of hazard levels at 5% and 20% probabilities of exceedence are also used in the analysis. Each of the two additional sets of ground motions had 25 three-component ground motion records, derived following the selection criteria given in Baker *et al.* (2011). Figure 2 compares: (i) uniform hazard spectra with the median pseudo-acceleration response spectra for the selected ground motions at five considered hazard levels [Fig. 2(a)] and (ii) median pseudo-acceleration response spectra for the selected ground motions at 10% in 50-year and 2% in 50-year hazard level events with the spectra for the code design basis earthquake (DBE) and MCE [Fig. 2(b)]. There is a good agreement between uniform hazard spectrum, median pseudo-acceleration response spectra, and design spectra for the range of periods the two considered structural systems would have during an earthquake event (greater than the fundamental period of the HP-SMRF, $T = 0.67$ sec).

4. Analysis-Model and Methods

To simplify the analysis for this study, time history analyses were performed on appropriately modeled two-dimensional (2D) frames utilizing OpenSees (McKenna and Fenves, 2004). This simplification is valid as the lateral load resisting frames are located only on the perimeter of the building and do not have common elements. Gravity-load-only type connections were used elsewhere in the structure. Details of numerical models and modelling assumptions are described in Terzic *et al.* (2014a). In short, (i) floor slabs were assumed to be axially inextensible, (ii) all elements of the two moment resisting frames were modeled utilizing force-based beam-column elements of OpenSees, (iii) isolators were modeled with zero-length elements (horizontal springs), one beneath each column of the structural frame, and tri-linear uniaxial material representative of a hysteretic behaviour of triple pendulum friction bearing, (iv) P- Δ effects from the gravity columns were accounted for by using single leaning column, (v) the effects of large deformations of beam and column elements were accounted for utilizing P- Δ nonlinear geometric transformation, (vi) damping was assigned to the frames using Rayleigh damping model and the damping ratio of 3%, (vii) the frames were subjected to horizontal and vertical components of ground motions.

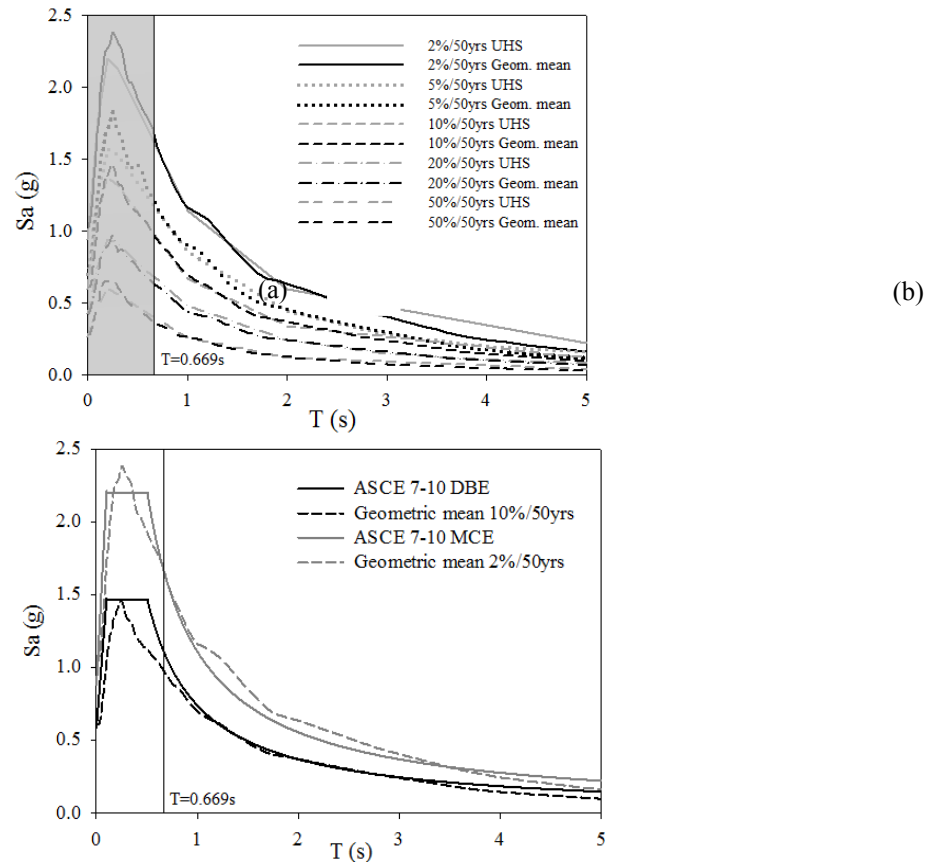


Fig. 2. Comparison of: (a) uniform hazard spectra with the median pseudo-acceleration response spectra for the selected ground motions at five considered hazard levels (2%, 5%, 10%, 20%, and 50% probabilities of exceedence in 50 years) and (b) median pseudo-acceleration response spectra for the selected ground motions at 10% in 50-year and 2% in 50-year hazard level events with the spectra for the code design basis earthquake (DBE) and maximum capable event (MCE). There is a good agreement between considered spectra for the periods greater than 0.67sec, the two considered systems would have for an earthquake event.

5. Comparison of structural response

While numerous parameters need to be considered to evaluate structural response fully, it is common to correlate performance to engineering demand parameters (EDP) based on story drifts, floor accelerations, and residual drifts. By comparing the average peak values of these EDPs for the five considered hazard levels, the relative performance characteristics of the systems can be assessed. The severity of damage to various structural and nonstructural components associated with these EDPs can be quantitatively assessed using fragility relations from FEMA P-58 (FEMA, 2012). Losses associated with this damage will be evaluated in the next section.

Base-isolated moment frame substantially reduces accelerations and drifts compared to the fixed-base frame (Figs. 3 and 4). While the effectiveness of the isolation system in reducing the story drifts increases with the increase of intensity of ground shaking (ranging from 20% to 62% with an average of 49%), the reduction of acceleration is consistently high at all hazard levels (ranging from 84% to 90% with an average of 88%). The BI-IMRF, with the uniform acceleration profile over the height of the building and the peak median value reaching 0.22g at the 2% in 50-year hazard level, most likely will not trigger any damage of the acceleration sensitive components (e.g., ceiling, MEP, contents). Figure 5 shows that isolation system is also effective in eliminating residual drifts of the moment frame at the higher hazard levels. At the 50% in 50-year hazard level, the HP-SMRF develops maximum median drift of 0.46%, 20% larger than maximum median drift of the BI-IMRF of 0.37% [Fig. 3(a)]. Because both moment frames are expected to yield at drift ratios slightly larger than 1%, elastic structural

behavior is anticipated at this hazard level. The damage to interior partitions is expected for both the HP-SMRF and BI-IMRF system, since the median drift associated with initiation of damage to partition walls commonly used in healthcare facilities and schools is 0.21% (FEMA, 2012). Median horizontal accelerations in the HP-SMRF range from 0.26g to 0.67g over the height of the building [Fig. 4(a)], likely triggering damage to piping, electronic and medical equipment in the upper levels (FEMA, 2012).

At the 20% in 50-year hazard level, greater differences in story drift demands were observed between the two systems [Fig. 3(b)]. Compared to the BI-IMRF, the fixed-base HP-SMRF had about 2 times larger drift ratio at every level, with the peak median value reaching 0.84%. This would likely result in a greater damage to partition walls and initiation of damage to stairs (that initiates at drift of 0.5%, per FEMA 2012). At this hazard level, damage to structural elements is not anticipated. Median horizontal accelerations in the HP-SMRF range from 0.37g to 1.13g over the height of the building [Fig. 4(b)]. These accelerations extend the regions of the building that undergoes acceleration-related damage, and trigger additional damage to ceilings, chillers, fire sprinkler drops, bookcases, and filing cabinets (FEMA, 2012). At the 10% in 50-year hazard level, Figure 3(c) shows even greater differences in story drift demands between the two systems [Fig. 3(b)]. The fixed-base HP-SMRF had the peak median drift ratio of 1.24%, which suggests initiation of yielding of the system and probable extensive damage to wall partitions and moderate damage to stairs. The BI-IMRF, with the peak median drift ratio of 0.57% is anticipated to remain elastic with slight damage to wall partitions and stairs. Median horizontal accelerations in the HP-SMRF ranged from 0.59g to 1.54g over the height of the building [Fig. 4(c)]. These accelerations extend the regions of the building that undergoes acceleration-related damage observed at lower hazard levels, and trigger additional damage to lightening, cooling tower, HVAC ducts, and air handling units.

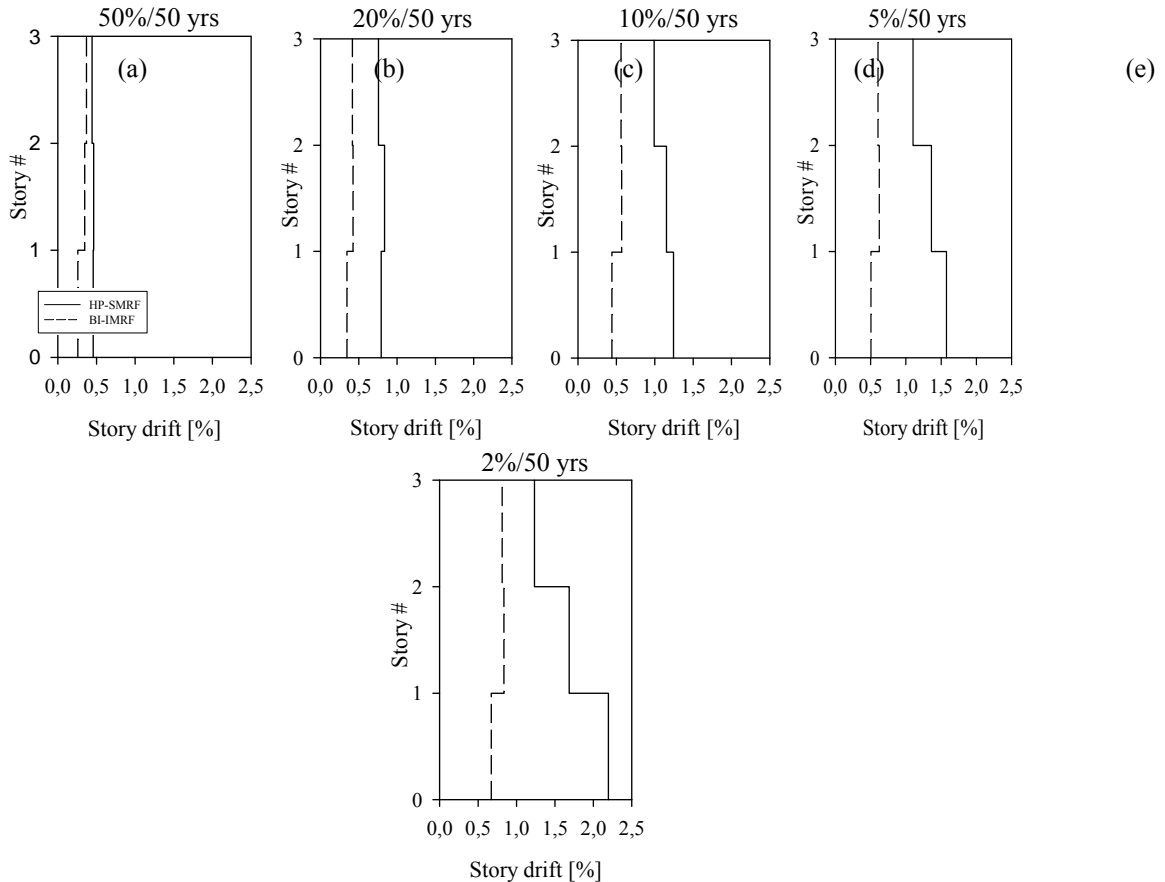


Fig. 3. Median story drifts of the HP-SMRF and the BI-IMRF on TFPBs for five hazard levels: 2%, 5%, 10%, 20%, and 50% probabilities of exceedence in 50 years.

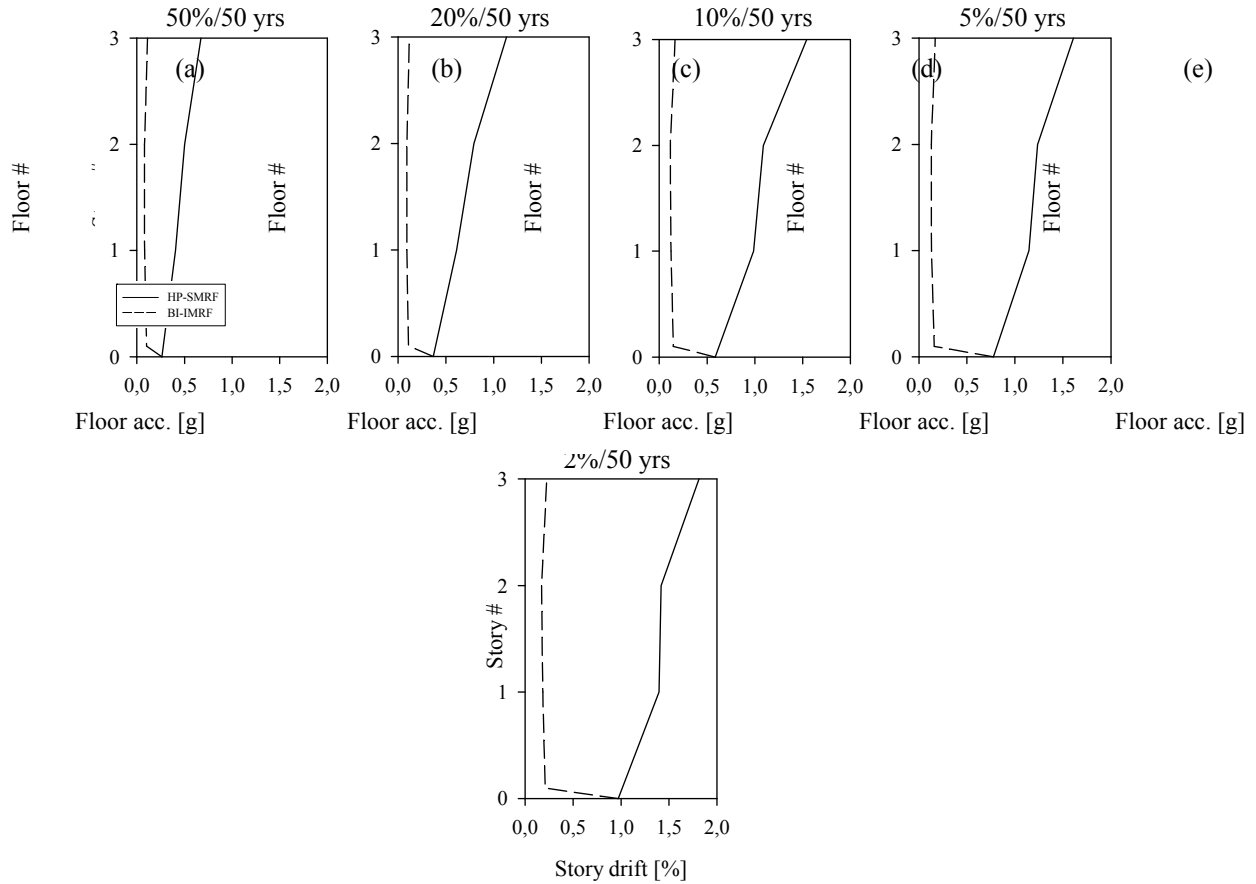


Fig. 4. Median absolute floor accelerations of the HP-SMRF and the BI-IMRF on TFPBs for five hazard levels: 2%, 5%, 10%, 20%, and 50% probabilities of exceedence in 50 years.

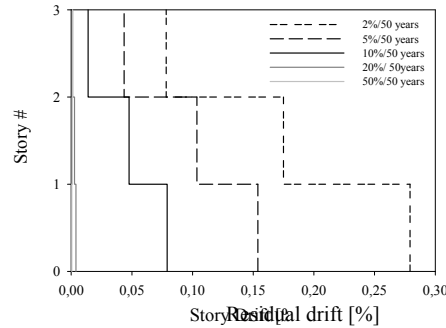


Fig. 5. Residual story drifts of the HP-SMRF at five hazard levels. Superstructure of the BI-IMRF had no residual drifts.

At the 5% and 2% in 50-year hazard levels, the fixed-base HP-SMRF had median peak story drifts of 1.57% (5% in 50 years) and 2.24% (2% in 50 years) (Figs. 3d,e), suggesting damage to both structural and nonstructural components, requiring substantial repair. The BI-IMRF, with the peak median drift ratios of 0.62% (5% in 50 years) and 0.83% (2% in 50 years) is anticipated to remain elastic with slight non-structural damage. Median horizontal accelerations in the HP-SMRF range from 0.78g to 1.61g for the 5% in 50-year hazard level and from 0.97g to 1.81g for the 2% in 50-year hazard level (Figs. 4d,e), causing damage to all acceleration sensitive non-structural components and content except for the electrical systems and components.

6. Loss analysis

Two loss metrics used to estimate effectiveness of isolation system in reducing the total financial losses are: (1) financial losses associated with the cost required to implement repairs and (2) repair time. The computer software Performance Assessment Calculation Tool (PACT) (ATC, 2012) is used to calculate repair costs and repair times for the two systems (fixed-base and base-isolated moment frames) and two occupancy types (healthcare and school), at each of five considered hazard levels. In PACT, each building component and content is associated with a fragility curve that correlates EDPs to the probability of that item reaching a particular damage state. The component's damage is then related to a loss (e.g., repair cost or repair time) utilizing consequence functions. The total loss at a hazard level is then estimated by integrating losses over all components of a system. To account for the many uncertainties affecting calculation of seismic performance, the *FEMA P-58* methodology uses a Monte Carlo procedure to perform loss calculations (FEMA, 2012). The type and quantities of most non-structural components and contents used in the loss analysis were determined using the normative quantities recommended by *FEMA P-58* (FEMA, 2012). The components considered in this study included: (i) structural: moment connections, shear tab gravity connections, base plates, and column splices, (ii) non-structural: partition walls, curtain walls, cladding, ceiling, lighting, stairs, elevators, and MEP components, and (iii) content: bookcases, filing cabinets, computers, servers, and medical equipment. Isolator devices and utilities at the isolation level are not included in the loss model due to unavailability of their fragility functions in PACT. For the healthcare occupancy, the fragility functions for the medical equipment (not available in PACT) are adopted from Yao and Tu (2012). These fragility functions are derived by investigating 41 healthcare buildings in the aftermath of the 1999 Chi-Chi earthquake. The consequence functions, relating damage of medical equipment to the repair cost, are developed based on an estimate that the medical equipment cost is 44% of the total building cost (Taghavi and Miranda 2003). The consequence functions, relating damage of medical equipment to the repair time, were not developed due to unavailability of data.

Replacement costs for the buildings, which are input for the loss analysis with PACT, are equal to the initial construction cost increased by 20% to include cost allowances for demolition and site clearance (FEMA, 2012). The initial construction costs of the school are estimated to be \$17,823,000 for the HP-SMRF and \$17,408,000 for the BI-IMRF, the same as if it was a commercial building (Terzic *et al.* 2014a; Ryan *et al.* 2010). The initial construction cost of the healthcare facility was calculated using the metric of \$597.7/ sq ft (estimate by M. Phipps per Mayencourt, 2013). Considering the footprint of the three-story building, the initial construction cost of the healthcare is estimated to be \$38,730,960, the same for the two considered structural systems.

6.1. Repair Costs

Repair cost estimates can provide the design engineer with valuable insights regarding the desirability and cost-effectiveness of enhancements to the structural system. Figure 5 shows the median repair costs for the fixed-base and base-isolated moment frames for the five considered hazard levels and the two occupancy types: healthcare and school. It clearly shows effectiveness of base-isolated system in mitigating damage. Reduction in cost of damage repair is consistently high at all hazard levels for the both occupancy types. For the healthcare occupancy the reduction in repair cost ranges from 76% to 88% with an average of 85%, and for the school it ranges from 66% to 82% with an average of 76%. Cost of damage repair is several magnitudes higher for the healthcare (more expensive facility) than for the school (Fig. 5). Healthcare facility, whose initial cost is double of the school cost, has 3-4 times greater losses than the school if the fixed-base HP-SMRF is utilized, and about 2 times greater losses if the BI-IMRF is utilized. While the fixed-base system generates disproportionately greater losses for the more expensive facility, the base-isolated system generates proportionally greater losses.

To identify the major contributors to the losses, the total repair cost is disaggregated into structural components, non-structural components, and contents (Fig. 5). Non-structural components and content of the healthcare facility dominate the losses. In the case of the fixed-base healthcare facility, non-structural components dominate the losses (72% contribution) at the lower hazard levels (50% and 20% in 50 years). At the 10% and 5% in 50-year hazard levels, non-structural components and content have almost equal contribution to the total repair cost. At the 2% in 50-year hazard level, damage to the medical equipment, which is the primary source of the content damage, dominates the losses (71% contribution). For the fixed-base school, the base-isolated school, and the base-isolated

healthcare facility, nonstructural components dominate the losses (contribution greater than 73%), but to a smaller extent for the base-isolated buildings. Cost of damage repair of structural components, although minor for the fixed-base system at higher hazard levels (up to 23% for the school occupancy), is completely diminished through utilization of the base-isolation. To facilitate decision on whether to repair or replace a building damaged in an earthquake, repair costs can be expressed in terms of loss ratio, which *FEMA P-58* defines as the necessary repair costs divided by the building’s replacement costs. The building’s replacement cost in this case is based on the initial construction cost associated with the building’s structural and nonstructural components; the contents are excluded. According to *FEMA P-58* (FEMA, 2012), building owners typically elect to replace a building rather than repair it when the loss ratio exceeds 40%; however, other replacement triggers may also be used. Figure 6 plots loss ratios for each system at the five considered hazard levels.

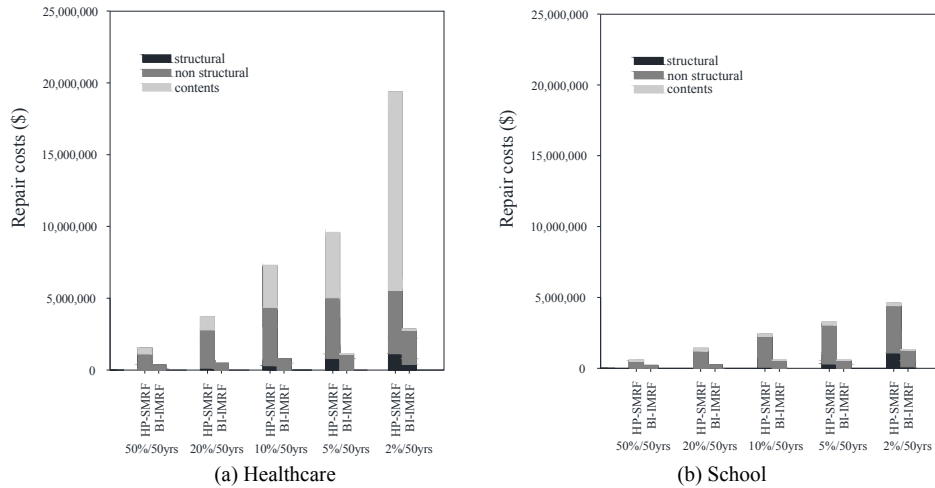


Fig. 5. Median repair costs for the HP-SMRF and the BI-IMRF for five hazard levels: 2%, 5%, 10%, 20%, and 50% probabilities of exceedance in 50 years.

Although the fixed-base healthcare and school buildings have significantly higher loss ratios than the base-isolated buildings at all hazard levels, the highest loss ratio of the fixed-base system of 0.26 is significantly smaller than the *FEMA P-58* replacement threshold of 0.4. Therefore, none of the buildings is to be replaced even for a very rare earthquake with the 2% probability of exceedance in 50 years.

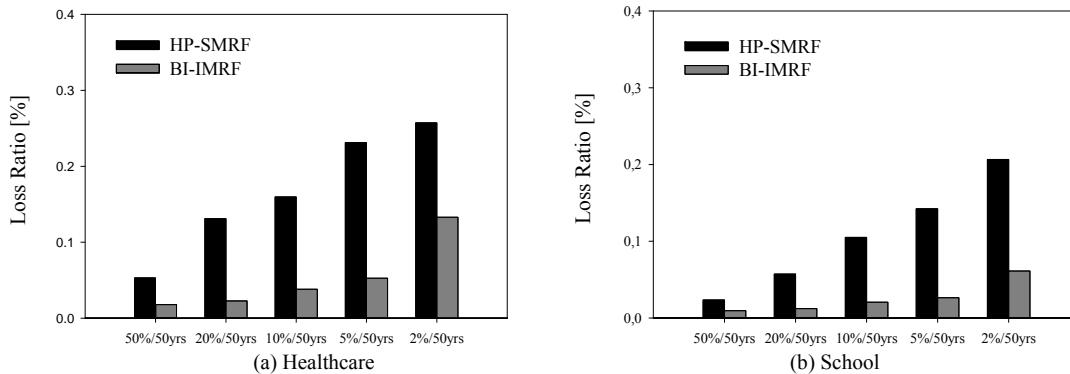


Fig. 6. Median loss ratio for the HP-SMRF and the BI-IMRF for five hazard levels and two occupancy types: (a) healthcare and (b) school.

6.2. Repair Time

To estimate the resilience of the system and the revenue losses resulting from the business interruption following an earthquake event, business downtime as a function of time needs to be characterized. Business downtime should include the time required to: (1) identify damage, design repairs or upgrades, obtain permits and financing, and to mobilize supplies and manpower; and (2) make the repairs necessary to restart operations. Although business models exist for the commercial occupancy type (e.g., Terzic *et al.* 2014a) such model could not be found for a school or a healthcare facility. Therefore, the study presented herein will use repair time as a metric for comparing the two systems and two occupancy types. Estimating the time required to repair a structure is difficult without specific information about the availability of workers and material. To calculate repair time, a number of assumptions are made. It is assumed that supplies and workers are available to permit necessary work. A high density of workers (one worker per 500 ft²) is used assuming that the building will not be occupied during the repair of damaged building components. The repair time is calculated considering two repair schemes: (1) *parallel* scheme that assumes simultaneous repair at all three floors, and (2) *serial* scheme that assumes sequential repair at three floor levels (FEMA, 2012). Both repair schemes assume sequential repair of all damaged components within one floor level. These repair schemes are not optimal but provide a good estimate of the lower and upper bound of the repair time for the chosen density of workers. While the assumptions made may be feasible for the systems with the smaller extent of damage (i.e., isolated system), they may be hard to achieve for the systems with more extensive damage (i.e., the fixed-base system). Therefore, these assumptions are advantageous for the HP-SMRF relative to the base isolated system as they reduce relative benefits of the isolated system. This is in line with the goal of this comparative study: that is estimation of minimum benefits of the isolated system in reducing the potential losses. Figure 7 shows the median repair times for the HP-SMRF and the BI-IMRF for five hazard levels, for the school and the healthcare facility, considering two repair strategies, parallel and serial. Base-isolation is again very effective in reducing the repair time, which also implies significantly smaller downtime of the isolated buildings. Upper (serial) and lower (parallel) bounds of the repair times are both several magnitudes smaller for the isolated buildings relative to the fixed-base buildings. For the 50% in 50-year hazard level, the repair times of the base-isolated buildings are 2-3 times smaller than for the fixed-base buildings. For the higher hazard levels, 20%, 10, and 5% in 50 years, the base-isolation is even more effective, resulting in 4-6 times smaller repair times. For the 2% in 50-year hazard level, the reduction in repair time is 3-4 times which is still significant.

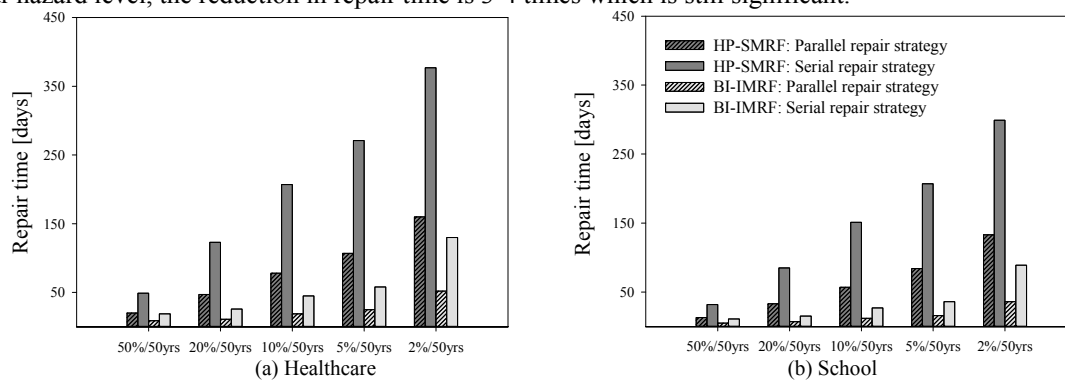


Fig. 7. Median repair times for the HP-SMRF and the BI-IMRF for five hazard levels and two occupancy types: (a) healthcare and (b) school, considering two repair strategies, parallel and serial.

While repair costs were significantly larger for the fixed-base healthcare facility than for the school, their repair times are of the same order of magnitude (Fig. 7). This is due to the fact that the repair time of the medical equipment was not included in the loss analysis. If the repair time of the medical equipment was included in the loss analysis, greater difference between repair times of the school and the healthcare facility, and also between the fixed-base and the base-isolated healthcare facility would be anticipated.

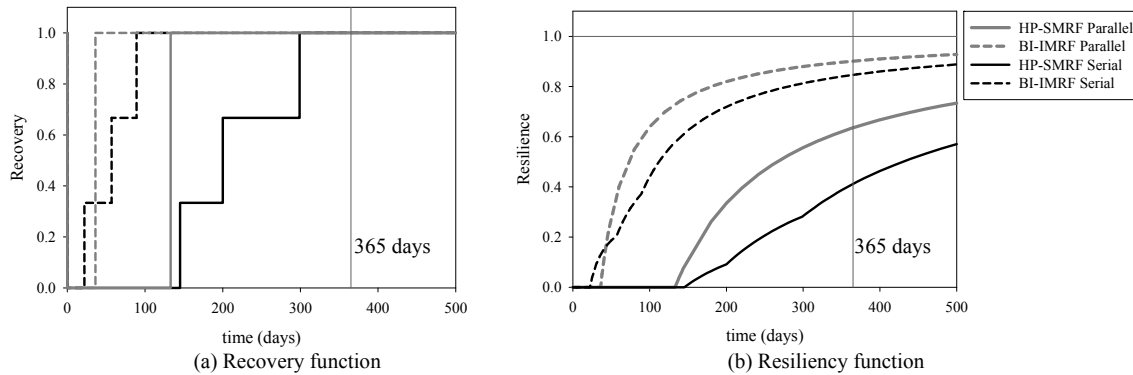


Fig. 8. Recovery and resiliency functions of the HP-SMRF and the BI-IMRF considering school occupancy and the 2% in 50-year hazard level.

7. Resiliency

Resiliency is the ability of a system to re-establish its function following a hazard event. The level of resiliency is measured by integrating the recovery function of the system within a certain period of time (Cimellaro et al, 2010a, b). To quantify the resiliency of the considered building, recovery function needs to be known. For the considered systems, it can be easily observed that the base-isolated buildings are more resilient than the fixed-base buildings as they have significantly smaller repair times and will therefore recover faster. However, to better quantify resiliency an attempt is made towards developing resiliency functions considering school occupancy and a very rare earthquake with a 2% probability of exceedence in 50 years. For this hazard level, it is assumed that both the fixed-base and the base-isolated system incur enough damage to trigger buildings closure. The probable lower and upper bounds for the recovery and therefore resiliency are established based on the lower (parallel scheme) and upper (serial scheme) bounds of repair times. Figure 8 clearly shows significantly greater resiliency of the base-isolated relative to the fixed-base system. While the fixed-base system starts to re-establish its function between 133 and 145 days following a very rare earthquake, the base-isolated system starts to recover its function way earlier – between 22 and 36 days. Resiliency functions (Fig. 8(b)) are much steeper for the base-isolated school building, indicating faster recovery. Considering the recovery time frame of 365 days, resiliency factor for the fixed-base school is anticipated to be between 0.41 and 0.63, while it is substantially higher for the base-isolated building and is between 0.85 and 0.9.

8. Conclusions

Over the past two decades, performance-based earthquake evaluation has developed to a point where it can be effectively used in the design of structures. In particular, it can identify the contributions of different structural and nonstructural elements and contents to the total cost of ownership over the life span of a building, thereby enabling the designer to enhance a given design or choose alternative structural systems to improve performance and mitigate damage. For a healthcare facility and a school building located in Oakland (California), the base-isolated system provide significant median damage savings and repair time reduction compared to the fixed-base system. This stems from the substantial reduction in accelerations, drifts, and residual drifts when isolated system is utilized at the base of the building. For the healthcare occupancy the reduction in repair cost ranges from 76% to 88% with an average of 85%, and for the school it ranges from 66% to 82% with an average of 76%. Such big reduction in cost of damage repairs of base-isolated systems comes primarily from preventing damage of the expensive equipment and structural components, and from minimizing the damage of non-structural components. Repair times are 3-6 times smaller for the isolated buildings relative to the fixed-base buildings. For the design basis earthquake (10% probability of exceedence in 50 years) and healthcare occupancy, the repair time of the fixed-base building is expected to be in the range of 78 and 207 days, while it is in the range of 19 and 45 days for the base-isolated

building. Such dramatic reduction in repair time implies significantly smaller downtime and higher resilience of the base-isolated buildings. The work presented here is indicative of the effectiveness of the base isolation in mitigating damage and associated losses. However, additional studies should be carried out to better characterize facility's downtime, business interruption costs, and resilience. Additional work is also needed to improve fragility and consequence functions of healthcare and school equipment.

Acknowledgements

The research leading to these results has received funding from the Pacific Earthquake Engineering Research Center and the European Community's Seventh Framework Program - Marie Curie International Reintegration Actions - FP7/2007-2013 under the Grant Agreement n° PIRG06-GA-2009-256316 of the project ICRED - Integrated European Disaster Community Resilience, and by the Marie Curie International Outgoing Fellowship (IOF) Actions-FP7/2007-2013 under the Grant Agreement n°PIOF-GA-2012-329871 of the project IRUSAT—Improving Resilience of Urban Societies through Advanced Technologies.

References

- American Institute of Steel Construction (AISC), 2005. "Prequalified Connections for Special and Intermediate Steel Moment Frames for Seismic Applications," ANSI/AISC 358-05, Chicago, IL.
- American Society of Civil Engineers (ASCE), 2010. "Minimum Design Loads for Buildings and Other Structures," ASCE 7-10, Reston, VA.
- Applied Technology Council (ATC), 2012. Performance Assessment Computation Tool (PACT). Applied Technology Council, Redwood City, CA.
- Baker, J. W., Lin, T., Shahi, S. K., and Jayaram, N., 2011. New ground motion selection procedures and selected motions for the PEER transportation research program. Pacific Earthquake Engineering Research Center, University of California, Berkeley, CA, USA. Report PEER 2011/03.
- Cimellaro, G. P., Reinhorn, A. M., and Bruneau, M., 2010a. "Framework for analytical quantification of disaster resilience." *Engineering Structures*, 32(11), 3639–3649.
- Cimellaro, G. P., Reinhorn, A. M., and Bruneau, M., 2010b. "Seismic resilience of a hospital system." *Struct. and Infrastruct. Eng.*, 6(1-2), 127-144.
- ICC IBC, 2012. "International Building Code", International Code Council.
- FEMA, 2012. Next-Generation Methodology for Seismic Performance Assessment of Buildings, prepared by the Applied Technology Council for the Federal Emergency Management Agency, Report No. FEMA P-58, Washington, D.C.
- Mayencourt, P., 2013. "Seismic Life Cycle Cost Comparison of a Frame Structure," Master Thesis, Department of Civil, Environmental and Geomatic Engineering Swiss Federal Institute of Technology Zurich (ETHZ).
- McKenna, F. and Fenves, G.L., 2004. "Open System for Earthquake Engineering Simulation (OpenSees)," PEER, Univ. of California, Berkeley, CA.
- Miranda, E., Taghavi, S., 2003. "Response Assessment of Nonstructural Building Elements" Pacific Earthquake Engineering Research Center, University of California, Berkeley, CA, USA. Report PEER 2003/05.
- Ryan K. L., Sayani P. J., Dao N. D., Abraik E., and Baez Y. M., 2010. Comparative life-cycle analysis of conventional and base-isolated theme buildings. 9th US National & 10th Canadian Conference on Earthquake Engineering, Toronto, Canada.
- Terzic, V., Mahin, S., Comerio, M., 2014a. "Using PBEE in Seismic Design to Improve Performance of Moment Resisting Frames by Base-Isolation," *Earthquake Spectra* (under review).
- Terzic, V., Mahin, S.A., Comerio, M.C., 2014b. "Comparative life-cycle cost and performance analysis of structural systems," Proceedings of the 10th National Conference in Earthquake Engineering, Earthquake Engineering Research Institute, Anchorage, AK, 2014.
- USGS, 2013. Seismic Hazard Analysis tools. U.S. Geological Survey. (<http://earthquake.usgs.gov/hazards/designmaps/grdmotion.php>)
- Yao, C., Tu, Y., 2012. "The generation of earthquake damage probability curves for building facilities in Taiwan," Proceedings of the International Symposium on Engineering Lessons Learned from the 2011 Great East Japan Earthquake, March 1-4, 2012, Tokyo, Japan.